Apo A-I inhibits foam cell formation in apo E–deficient mice after monocyte adherence to endothelium

Hayes M. Dansky,[1] Sherri A. Charlton,[1] Courtenay B. Barlow,[1] Minna Tamminen,[1] Jonathan D. Smith,[1] Joy S. Frank,[2] and Jan L. Breslow[1]

[1]Laboratory of Biochemical Genetics and Metabolism, The Rockefeller University, New York, New York 10021, USA
[2]Cardiovascular Research Laboratory, Department of Medicine and Physiology, University of California–
 Los Angeles School of Medicine, Los Angeles, California 90095-1760, USA

Address correspondence to: Jan L. Breslow, Laboratory of Biochemical Genetics and Metabolism,
The Rockefeller University, Box 179, 1230 York Avenue, New York, New York 10021, USA.
Phone: (212) 327-7700; Fax: (212) 327-7165; E-mail: breslow@rockvax.rockefeller.edu.

We have previously shown that expression of the human apo A-I transgene on the apo E–deficient background increases HDL cholesterol and greatly diminishes fatty streak lesion formation. To examine the mechanism, prelesional events in atherosclerotic plaque development were examined in 6- to 8-week-old apo E–deficient and apo E–deficient/human apo A-I transgenic mice. A quantitative assessment of subendothelial lipid deposition by freeze-fracture and deep-etch electron microscopy indicated that elevated apo A-I did not affect the distribution or amount of aortic arch subendothelial lipid deposits. Immunohistochemical staining for VCAM-1 demonstrated similar expression on endothelial cells at prelesional aortic branch sites from both apo E–deficient and apo E–deficient/human apo A-I transgenic mice. Transmission electron microscopy revealed monocytes bound to the aortic arch in mice of both genotypes, and immunohistochemical staining demonstrated that the area occupied by bound mononuclear cells was unchanged. Serum paraoxonase and aryl esterase activity did not differ between apo E–deficient and apo E–deficient/human apo A-I transgenic mice. These data suggest that increases in apo A-I and HDL cholesterol inhibit foam cell formation in apo E–deficient/human apo A-I transgenic mice at a stage following lipid deposition, endothelial activation, and monocyte adherence, without increases in HDL-associated paraoxonase.

J. Clin. Invest. **104**:31–39 (1999).

Introduction

There is a strong inverse correlation between HDL cholesterol (HDL-C) and the incidence of coronary heart disease. The mechanisms by which elevated HDL-C reduces cardiovascular risk are not well understood. Three principal hypotheses have been proposed to explain the antiatherogenic role of HDL: (a) promotion of reverse cholesterol transport; (b) direct protection of the vessel wall or inhibition of lipoprotein oxidation; or (c) a marker for decreased levels of atherogenic lipoproteins.

Most experimental studies designed to test these hypotheses have used in vitro systems to evaluate the properties of HDL particles Studies have demonstrated that HDL particles can affect cholesterol efflux from cultured cells (1), interfere with LDL binding to extracellular matrix (2), inhibit adhesion molecule expression on cultured endothelial cells (3), and inhibit copper and cellular oxidation of lipoproteins (4). However, there is little direct evidence that HDL performs these functions in vivo.

Recently, transgenic and knockout mice with altered lipoprotein metabolism and atherosclerosis susceptibility have provided insight into the role of HDL in atherosclerosis. Two independent studies (5, 6) provide strong evidence that HDL has a direct effect on lesion formation. In these studies, apo E–deficient (E0) mice (7, 8), which develop foam cell and fibroproliferative lesions histologically similar to human atherosclerosis (9, 10), were bred with human apo A-I transgenic (hA-I) mice (11, 12). Increasing HDL-C 2-fold resulted in a 5- to 20-fold reduction in foam cell lesion area in 12- to 16-week-old apo E/human apo A-I transgenic (E0/hA-I) mice (5, 6). In addition, in 32-week-old mice, there was a strong inverse relationship between atherosclerotic lesion area and HDL-C that was independent of the level of non–HDL-C (5). These experiments demonstrate that elevated levels of HDL-C directly inhibit atherosclerosis and are not merely markers of decreased levels of atherogenic lipoproteins.

Previous studies in apo E–deficient mice have demonstrated that prelesional events include lipid retention (13), endothelial expression of VCAM-1 (14), and monocyte binding to arterial branch sites (9). In the present in vivo study, we compared these prelesional events and the activity of serum paraoxonase, an HDL-associated antioxidant enzyme. Our data demonstrate that elevated apo A-I and HDL-C inhibit atherogenesis in E0 mice at a stage following lipid deposition, endothelial activation, and monocyte adherence — without affecting serum paraoxonase activity.

Table 1
Lipid deposition in the intima of apo E–deficient mice

	Genotype	Number of micrographs examined	Total number of grid squares counted	Number of grid squares that contain lipid particles
Group I	C57 E0	30	486	169
	C57 E0/hA-I	30	476	148
Group II	E0	27	431	183
	E0/hA-I	34	557	167

Photographs (×22,949) were taken from deep-etched replicas of mouse aorta. A transparent grid containing 16 rectangles (area of each rectangle = 5.34 μm^2) was superimposed on the photos, and the rectangles were scored for the presence or absence of lipid without giving any weight to the amount of lipid present.

Methods

Mice. All mice were weaned at 3 weeks of age and fed a standard chow diet (PicoLab Rodent 20, catalog no. 5053, Ralston Purina Co. St. Louis, Missouri, USA: 20% protein from plant and animal sources, 4.5% wt/wt fat, 0.02% wt/wt cholesterol, no casein, no sodium cholate). All mice were housed in a specific pathogen-free environment. In some experiments, apo E–deficient mice (7) and apo E–deficient/human apo A-I transgenic mice (5) were obtained from an existing colony of mice at The Rockefeller University. These mice were of mixed genetic background and were first-generation littermates obtained from E0 × E0/hAI intercrosses. In 2 of the freeze-fracture experiments, C57BL/6 apo E–deficient mice (15) and C57BL/6 human apo A-I transgenic mice (12), obtained from The Jackson Laboratory (Bar Harbor, Maine, USA), were intercrossed to obtain C57BL/6 apo E–deficient, human apo A-I transgenic mice. For this experiment, first-generation littermates obtained from C57 E0 × C57 E0/hA-I intercrosses were used. In this paper, mice with the C57BL/6 background are designated as C57 to distinguish them from mice of mixed genetic background. The presence of the human apo A-I transgene was detected in plasma using a human apo A-I ELISA, as described below. E0/hAI mice with human apo A-I levels greater than 200 mg/dL, and their corresponding E0 littermates, were selected for this study. HDL-C was measured on a subset of the mice as previously described (16). HDL-C was 2-fold higher in E0/hAI mice when compared with E0 mice (mean ± SE: 71 ± 3, n = 19 vs. 34 ± 2, n = 16; P < 0.0001).

Human apo A-I ELISA: *measurement of apo A-I.* Mouse anti-human apo A-I mAb (BIODESIGN International, Kennebunk, Maine, USA), diluted 1:300 in bicarbonate buffer, was applied to wells of Nunc Maxisorb ELISA plates (Nalge Nunc International, Naperville, Illinois, USA) and incubated overnight at 4°C. All subsequent incubations were performed at room temperature with gentle agitation. Wells were washed with PBS and blocked with casein blocker (Pierce Chemical Co., Rockford, Illinois, USA) for 1 hour. Diluted standards (Diasorin Inc., Stillwater, Minnesota, USA) and plasma

samples, diluted 1:800,000 in casein/0.5% Tween-20, were applied to the wells for 1 hour. Plates were washed with PBS/Tween-20 (0.5%), and a 1:1,000 dilution of a goat anti-human apo A-I polyclonal antibody (BIODESIGN International) was applied for 1 hour. After washing, mouse anti-goat IgG (Pierce Chemical Co.) was applied for 1 hour. Horseradish peroxidase enzyme was detected by incubation with TurboTMB substrate (Pierce Chemical Co.). The reaction was terminated with 1 M sulfuric acid, and the absorbance was measured at 450 nm on a SpectraMax plate reader (Molecular Devices, Sunnyvale, California, USA).

Freeze-fracture and deep-etch electron microscopy. The heart with the attached aorta was rapidly removed from the animals and placed in an oxygenated phosphate-buffered Ringer's solution as described previously (13). Tissues pieces (2 × 1 mm) were removed from the aortic arch from selected sites as reported previously (13), placed endothelial side up on a moist filter paper over rectangles of gelatin, and ultrarapidly frozen on a highly polished liquid nitrogen–cooled copper block. Frozen pieces of aorta were fractured at –150°C at a vacuum of 1×10^{-7} in a Balzers 301 freeze-fracture apparatus (Balzers Instruments, Balzers, Lichtenstein). Deep-etched, rotary-shadowed replicas were generated as described previously (17, 18).

Photographs were taken of each replica. The only selection process was to photograph portions of the replica where the fracture plane passed through the intima. Each photo was taken at ×10,000. This enabled the observer to determine the level of the fracture plane but not the details of the matrix, thus ensuring that bias did not enter the data collection. Each negative was enlarged photographically to make the lipid particles visible in the matrix for scoring. A transparent grid containing 16 rectangles (area of each rectangle = 5.34 μm^2) was superimposed on the photos, and the rectangles were scored for the presence or absence of lipid. To determine whether the amount of lipid deposits in each area was affected by elevated apo A-I and HDL-C, 29 replicas were obtained from C57BL/6 E0/hA-I mice (n = 2), and 30 replicas were obtained from C57BL/6 E0 mice (n = 2). In these experiments,

Table 2
Quantitative assessment of subendothelial lipid in 6-week-old apo E–deficient mice

Genotype	Type 1	Type 2	Type 3
C57 E0	21	174	89
C57 E0/hA-I	35	194	82

Freeze-etch replicas were taken from the aorta arch of C57 E0 (n = 2) and C57 E0/hA-I (n = 2) mice. Areas within the intima that contained lipid were scored as follows: type 1, greater than half the area filled with aggregated lipid; type 2, more than 2 clusters of aggregated lipid in the area; and type 3, individual lipid particles dispersed in the area. Values are the total number of areas showing a given pattern of lipid deposition.
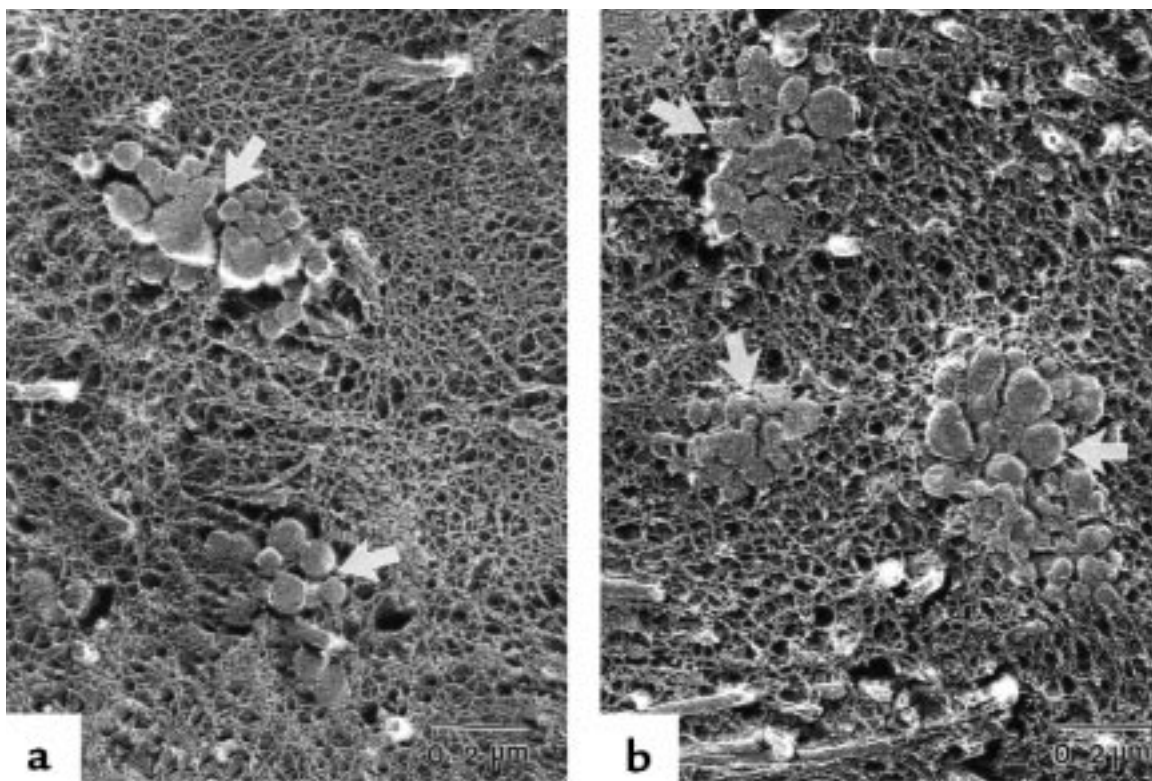
Figure 1
Freeze-etch electron micrographs from the intima of E0 (**a**) and E0/hA-I (**b**) mice. Arrows point to clusters of lipid within the matrix. This lipid configuration was quantified as type 2 for the data in Table 2. ×64,800.

only areas within the intima that contained lipid were scored. To quantify the amount of lipid present in the intima in both genotypes, each grid space was scored as follows: type 1, greater than half the area filled with aggregated lipid; type 2, more than 2 clusters of aggregated lipid in the area; and type 3, individual lipid particles dispersed in the area.

Transmission electron microscopy. Thin-section electron microscopy was performed on tissue taken from periodic sampling throughout the aortic arch. The aorta was dissected and freed from surrounding connective tissue, fixed in glutaraldehyde followed by osmium tetroxide, dehydrated in graded alcohol, and embedded in Epon as described previously (13). Cross-sections were cut to easily identify monocytes adhering to the endothelial cell wall. Two animals of each genotype were examined (10 tissues samples × 5 sections for 50 sections per aorta).

Immunohistochemistry. Mice were anesthetized, and blood was collected from left ventricular puncture into syringes containing EDTA. The circulatory system was perfused with 0.9% NaCl by cardiac intraventricular canalization. The heart and ascending aorta, including the aortic arch, were removed. The aortic root and aortic arch were frozen in OCT embedding medium using liquid nitrogen–cooled isopentane. OCT blocks were stored at –70°C until sectioned for immunocytochemistry.

Six-micrometer frozen aortic arch sections were cut and allowed to adhere to Fisher Plus slides. Eight-

micrometer aortic root sections were obtained from an anatomically defined area of the aortic root, starting with the appearance of the aortic valve leaflets and ending when the aortic leaflets were no longer visible. Sections were fixed with acetone for 5 minutes and were subjected to a 0.3% hydrogen peroxide incubation to block endogenous peroxidase activity, followed by blocking in normal rabbit serum. Primary antibody was applied for 90 minutes at room temperature. The following antibodies were used: rat anti-mouse VCAM-1 mAb (1:250; Southern Biotechnology Associates, Birmingham, Alabama, USA), rat anti-mouse IgG1 control antibody (1:250; Vector Laboratories, Burlingame California, USA), rat anti-mouse CD11a (1:1000; PharMingen, San Diego, California, USA). The sections were washed in PBS, and a biotinylated rabbit anti-rat, mouse-absorbed secondary antibody (1:200; Vector Laboratories) was applied for 45 minutes, followed by a wash and a 30-minute incubation with avidin-biotin complex linked to horseradish peroxidase (Vector-Elite; Vector Laboratories). For CD11a antibody staining, the signal was enhanced using a tyramide signal amplification kit as instructed by the manufacturer (NEN Life Science, Products Boston, Massachusetts, USA). Peroxidase was detected with 3-amino-9-ethylcarbazole (DAKO Corp., Carpinteria, California, USA). Controls were performed with either an irrelevant isotype-matched mAb or in the absence of primary antibody, and no background staining was seen.

Quantitation of CD11a-positive cells. Immunoperoxidase staining using the anti-CD11a antibody was used to detect adherent mononuclear cells. Pilot studies demonstrated that visual counting of immunoperoxidase-stained mononuclear cells was not reliable because mononuclear cells assume different shapes, depending upon whether the cell is adhered or in the process of spreading or undergoing transendothelial migration. Therefore, the area occupied by stained cells was quantified with a computer-assisted video capture system (Optimetrics, Bioscan, Inc., Edmonds, Washington, USA). The operator was blinded with respect to the animal genotype. The area occupied by bound mononuclear cells was measured on 1 section per slide, for a total of 5 slides per animal. The 5 areas were then averaged.

Measurement of aryl esterase and paraoxonase. Blood was obtained from the tail vein and collected in capillary tubes containing no anticoagulant. Mouse serum was diluted in PBS and added to microtiter plates. Phenyl acetate (aryl esterase; 1 mM) or paraoxon (paraoxonase; 1 mM) in 20 mM Tris buffer (pH 8) was added, and the change in OD 270 nm (aryl esterase) or OD 405 nm (paraoxonase) was measured in a kinetic assay for 2 minutes in a plate reader (Molecular Dynamics, Sunnyvale, California, USA) at room temperature. Relative aryl esterase and paraoxonase activities were expressed as the slope (Δ OD/s). All mouse samples for the aryl esterase and paraoxonase assays were measured simultaneously.

Statistics. Comparisons between groups were performed using an unpaired Student's *t* test.
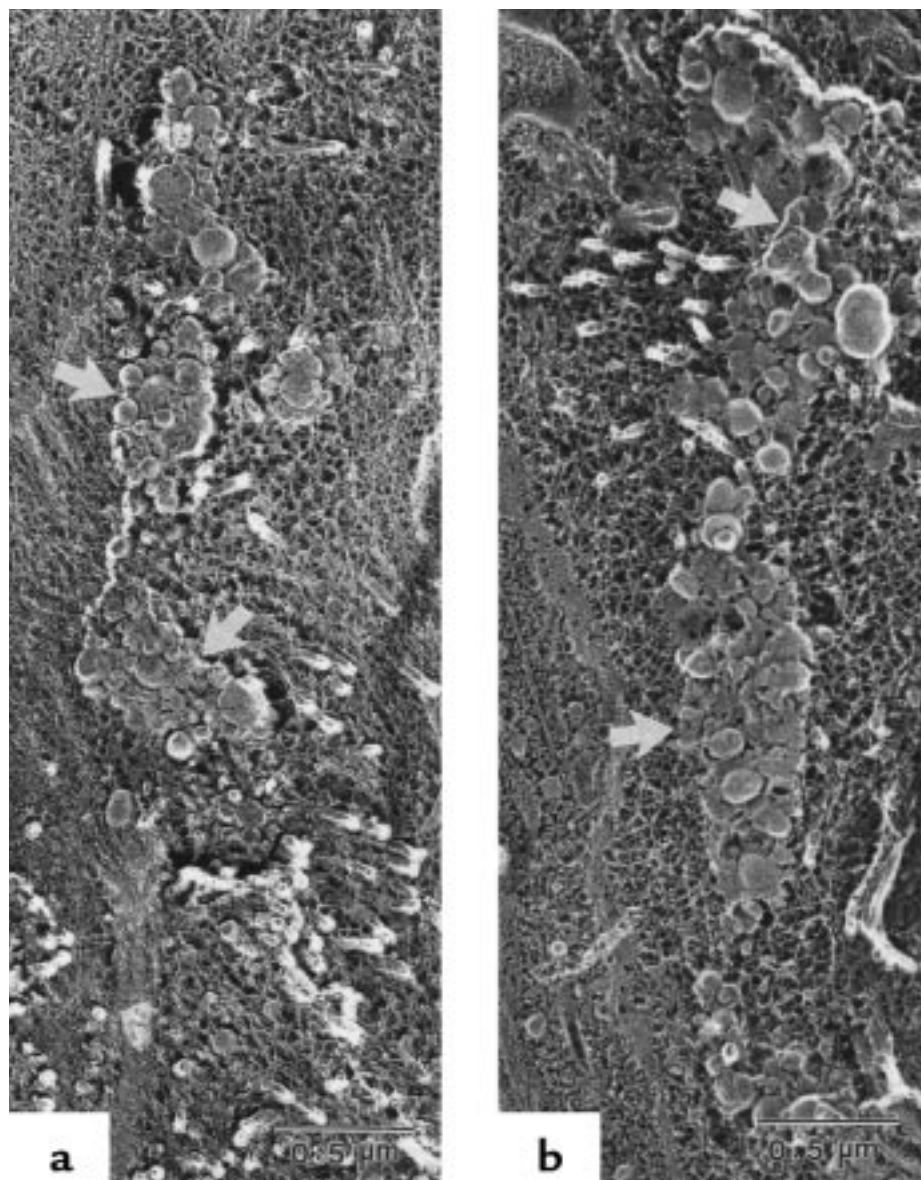
Figure 2
Freeze-etch electron micrographs from the intima of E0/hA-I (**a**) and E0 (**b**) mice. The arrows indicate large aggregates of lipid that course through the matrix filaments and collagen fibrils of the intima. This "vein" of aggregated lipid was quantified as type 1 deposition in Table 2. ×13,937.
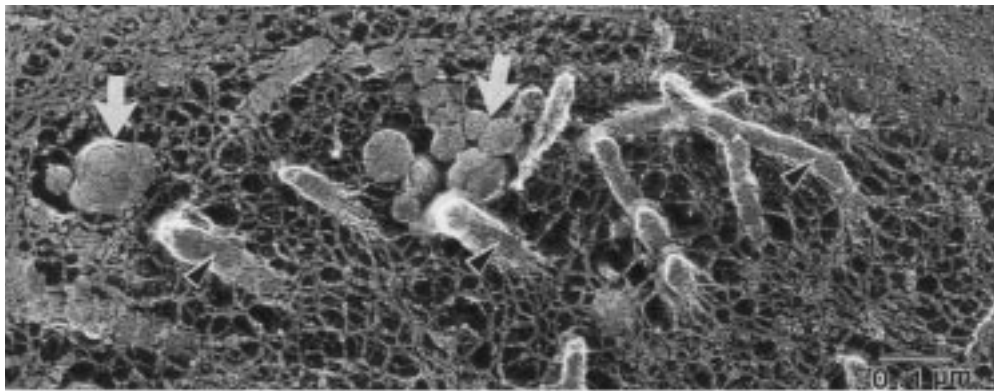
Figure 3
Freeze-etch electron micrograph from the intima of an E0 mouse. The arrow points to individual lipid particles in close association with collagen fibrils (arrowheads). This type of lipid deposition was quantified as type 3 in Table 2. ×97,200.

Results

A quantitative study was performed using freeze-fracture and deep-etch electron microscopy to determine whether elevated apo A-I would decrease subendothelial lipid retention in E0/hA-I mice. We have previously shown that lipid is retained in the subendothelial matrix as early as 3 weeks of age in apo E–deficient mice, whereas the subendothelial matrix of control (wild-type) mice contains no lipid deposits (13). Two groups of mice were sacrificed for the evaluation of subendothelial lipid deposition. The first group included 6-week-old C57 E0 (n = 2) and C57 E0/hA-I (n = 2) mice, and the second group contained 6-week-old E0 (n = 2) and E0/hA-I (n = 2) mice of mixed genetic background. The intima at branch sites in the aortic arch from both E0 and E0/hA-I mice from both genetic backgrounds had lipid associated with the matrix. The presence or absence of subendothelial lipid deposits, regardless of the amount or configuration of lipid in each area, was scored in a blind fashion. The number of areas containing lipid deposits was similar in E0/hA-I and E0 mice within both groups (Table 1). Lipid configuration occurred in 3 forms in both genotypes. The most frequent form was small clusters of aggregated lipid surrounded by matrix, especially collagen fibrils (Figure 1; Table 2, type 2). The least frequent form was the appearance of large aggregates that spread out in long veins between the matrix and the collagen fibrils (Figure 2; Table 2, type 1). The third lipid configuration, individual lipid particles dispersed in the intima, was of intermediate frequency (Figure 3; Table 2, type 3). Based on this semiquantitative scoring method, the amount of lipid in the intima was similar in the E0/hA-I and E0 mice at this age (Table 2).

Previous studies have demonstrated that VCAM-1 expression is induced in endothelial cells overlying lesion-prone aortic branch sites in the apo E–deficient mouse (14). To determine whether elevated apo A-I and HDL-C inhibit endothelial induction of VCAM-1, aortae from 8-week-old E0 (n = 4) and E0/hA-I mice (n = 4) of mixed genetic background were stained for endothelial VCAM-1. Endothelial cells at aortic branch sites in the aortic arch from both E0 and E0/hA-I mice stained positive for VCAM-1 (Figure 4). There were no qualitative differences in the intensity of endothelial VCAM-1 staining or the number of endothelial cells that stained positive for VCAM-1 in E0 and E0/hA-I mice.

The demonstration of VCAM-1 expression on endothelial cells does not fully address the issue of monocyte adherence because other adhesion molecules may be involved. Therefore, qualitative and quantitative assessments of monocyte adherence in situ were performed in E0 and E0/hA-I mice. Thin-section electron micrographs revealed monocytes bound to aortic branch sites from E0 and E0/hA-I mice (Figure 5). No apparent qualitative differences in monocyte binding were noted in the electron micrograph sections examined. A quantitative mononuclear cell adhesion assay was developed to determine if elevated apo A-I affects the number of mononuclear cells bound to lesion-prone areas. Previous examinations of the cells present in fatty streak lesions in E0 mice have demonstrated that the majority of cells are macrophages, with a small percentage being T lymphocytes (16, 19–21). Because commercially available anti-monocyte/anti-macro-phage antibodies (e.g., MOMA-2, Mac-3) stain macrophages in atherosclerotic lesions

Table 3
Oxidation-related parameters in apo E–deficient and apo E–deficient/human apo A-I transgenic mice

Genotype	Sex	n	Aryl esterase	Paraoxonase
C57BL/6 wild-type	Male	4	22 ± 0.6	15 ± 0.7
E0	Male	5	27 ± 2.2	15 ± 0.8
E0/hA-I	Male	5	26 ± 2.8	12 ± 1.0
C57BL/6 wild type	Female	4	34 ± 1.0	22 ± 1.1
E0	Female	5	29 ± 2.4	16 ± 1.4[A]
E0/hA-I	Female	5	28 ± 1.1	13 ± 1.4[B]

Values are expressed as mean ± SE. Unpaired Student's t test was used for comparisons between groups. Comparisons between E0 and wild-type mice: [A]P < 0.05, [B]P < 0.01.
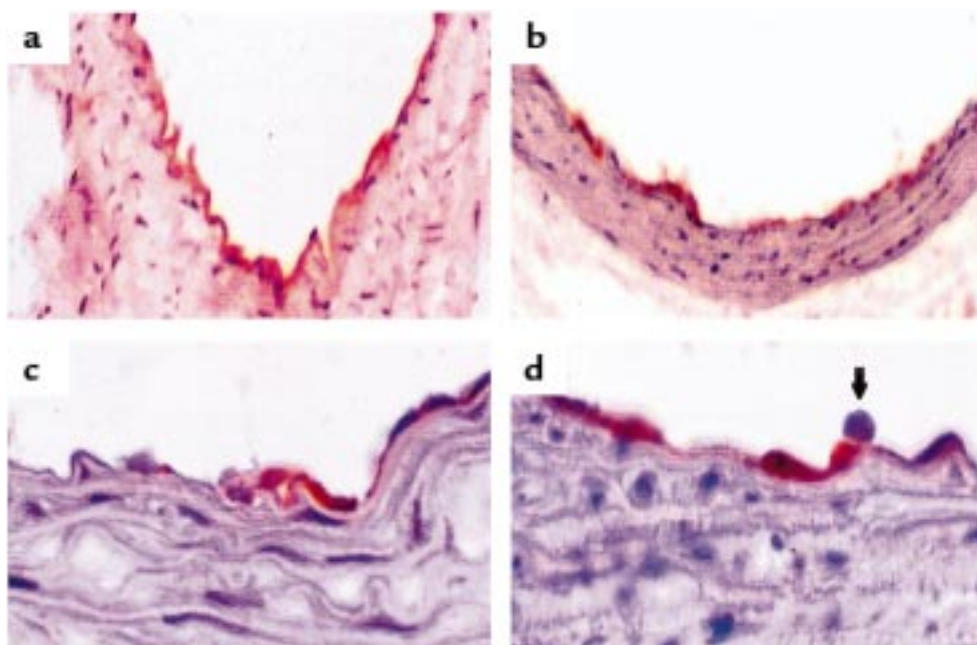
Figure 4
Aortic arch sections from 8-week-old E0 and E0/hA-I mice. (**a** and **c**) Apo E–deficient mouse aortic arch sections (E0); (**b** and **d**) human apo A-I transgenic, apo E–deficient mouse aortic arch sections (E0/hA-I). VCAM-1 antibody staining (red) for VCAM-1 at prelesional vascular branch points with ×10 objective (**a** and **b**) and oil objective (**c** and **d**). A mononuclear cell (arrow) is attached to an endothelial cell staining positive for VCAM-1 in **d**.

but do not detect adherent monocytes (H. Dansky et al., unpublished observations), an antibody to a cell surface integrin, CD11a, which is present on leukocytes and absent on endothelial and smooth muscle cells, was chosen. E0 and E0/hA-I mice were sacrificed at 8 weeks of age. Immunoperoxidase staining using the anti-CD11a antibody was performed to detect adherent leukocytes. As shown in Figure 6, CD11a antibody staining detected cells bound to the aortic root in both E0 and E0/hA-I mice. The area occupied by positive-stained mononuclear cells was measured in an anatomically defined area of the aortic root from 8-week-old E0 ($n = 7$) and HuAItgE0 ($n = 7$) mice. As shown in Figure 7, there were no significant differences in the area occupied by CD11a$^+$ cells in the aortic root of E0 and E0/hA-I mice.

Paraoxonase is an enzyme transported on HDL particles in humans and mice that has been shown to metabolize oxidized lipids in vitro. Serum paraoxonase levels were determined in outbred E0 and E0/hA-I mice, with both paraoxon and phenyl acetate as substrates. As noted in previous studies (4), there were decreases in paraoxonase and aryl esterase activity in female E0 mice when compared with wild-type control mice, but this difference was not noted in male mice (Table 3). There was an ~20% decrease in paraoxonase activity in male and female E0/hA-I mice compared with E0 mice, although this difference failed to reach statistical significance. This difference is opposite that which would have been expected if increased HDL resulted in increased paraoxonase activity.

Discussion
Mouse models of hypercholesterolemia and atherosclerosis have provided considerable insight into the pathogenesis of atherosclerosis. Studies using apo E–deficient mice and other murine models of hypercholesterolemia have demonstrated that early events in atherogenesis include the accumulation of lipoprotein aggregates in the subendothelial space (13), induction of endothelial VCAM-1 expression (14), monocyte adherence (9), and subsequent foam cell formation. Transgenic overexpression of human apo A-I increases HDL-C and dramatically inhibits atherosclerotic lesion formation at the early foam cell stage in apo E–deficient mice (5, 6). Therefore, it is likely that HDL particles exert their antiatherogenic effects in this model by blocking 1 or more steps leading to foam cell formation.

Pathological studies have demonstrated the presence of subendothelial lipid deposits prior to lesion development in a variety of animal models of hypercholesterolemia, including rabbits (17) and apo E–deficient mice (13). In vitro studies suggest that lipid retention by the vessel wall involves interactions between apo B and matrix proteoglycans (22). One study demonstrated that HDL particles can alter the subendothelial matrix proteoglycans and affect lipid binding to matrix in vitro (2). To our knowledge, before the present study, the effect of HDL particles on lipoprotein retention in vivo had not been examined. This study addresses whether elevated apo A-I and HDL-C affect lipoprotein retention by the vessel wall at lesion-prone areas. Because the amount of lipid retained by the vessel wall prior to the

influx of monocytes is minute and unlikely to be detected using traditional biochemical or structural assays, freeze-fracture and deep-etch electron microscopy were used because these methodologies have the resolution needed to see lipid particles the size of LDL and to retain the in vivo macromolecular structure of the intima. The human apo A-I transgene did not affect the number of intimal areas containing lipid in 2 separate experiments. In addition, elevated human apo A-I and HDL-C did not affect the amount of lipid deposited in each area, based on a semiquantitative assessment.

Endothelial VCAM-1 expression at lesion-prone areas was unchanged by the presence of high circulating HDL-C in the E0/hAI mouse. Oxidized LDL augments VCAM-1 expression on cytokine-stimulated endothelial cells (23, 24), whereas HDL and apo A-I inhibit cytokine-mediated induction of VCAM-1 on cultured endothelial cells (3, 25, 26). The differential effect of HDL-C on VCAM-1 expression in vivo versus in vitro may be related to the mechanism of VCAM-1 induction in the 2 systems. In vitro, VCAM-1 may be directly induced on endothelial cells by the presence of cytokines or bioactive oxidized phospholipids, such as lysophosphatidylcholine (27). The mechanism by which VCAM-1 is induced in vascular endothelial cells at lesion-prone areas in vivo may be related to hemodynamic alterations at vascular branch sites in the set-

ting of hypercholesterolemia (14). The pathway that leads to endothelial induction in vivo may differ markedly from cytokine-mediated induction of cultured endothelial cells.

Previous studies have clearly demonstrated that decreases in monocyte number or recruitment to the vascular wall have profound effects on atherogenesis. Foam cell formation is greatly diminished in apo E–deficient mice lacking either M-CSF (28, 29) or MCP-1 (30). Elevated HDL-C and apo A-I did not affect the total number of mononuclear cells bound to the aortic root of E0/hA-I mice, suggesting that the human apo A-I transgene does not alter initial monocyte recruitment to lesion-prone areas. However, our assay cannot evaluate differences in total monocyte recruitment over time.

Numerous studies suggest that lipoprotein oxidation is involved in the pathogenesis of atherosclerosis (31, 32). The majority of studies demonstrating that HDL can inhibit lipoprotein oxidation have been conducted in vitro. HDL particles can inhibit in vitro oxidation of LDL and cell-mediated oxidation in an aortic endothelial–smooth muscle cell coculture model (33). Navab et al have demonstrated that the paraoxonase enzyme carried on HDL particles is responsible for the inhibition of LDL oxidation in the aortic wall coculture model, and that targeted disruption of the paraoxonase gene in mice
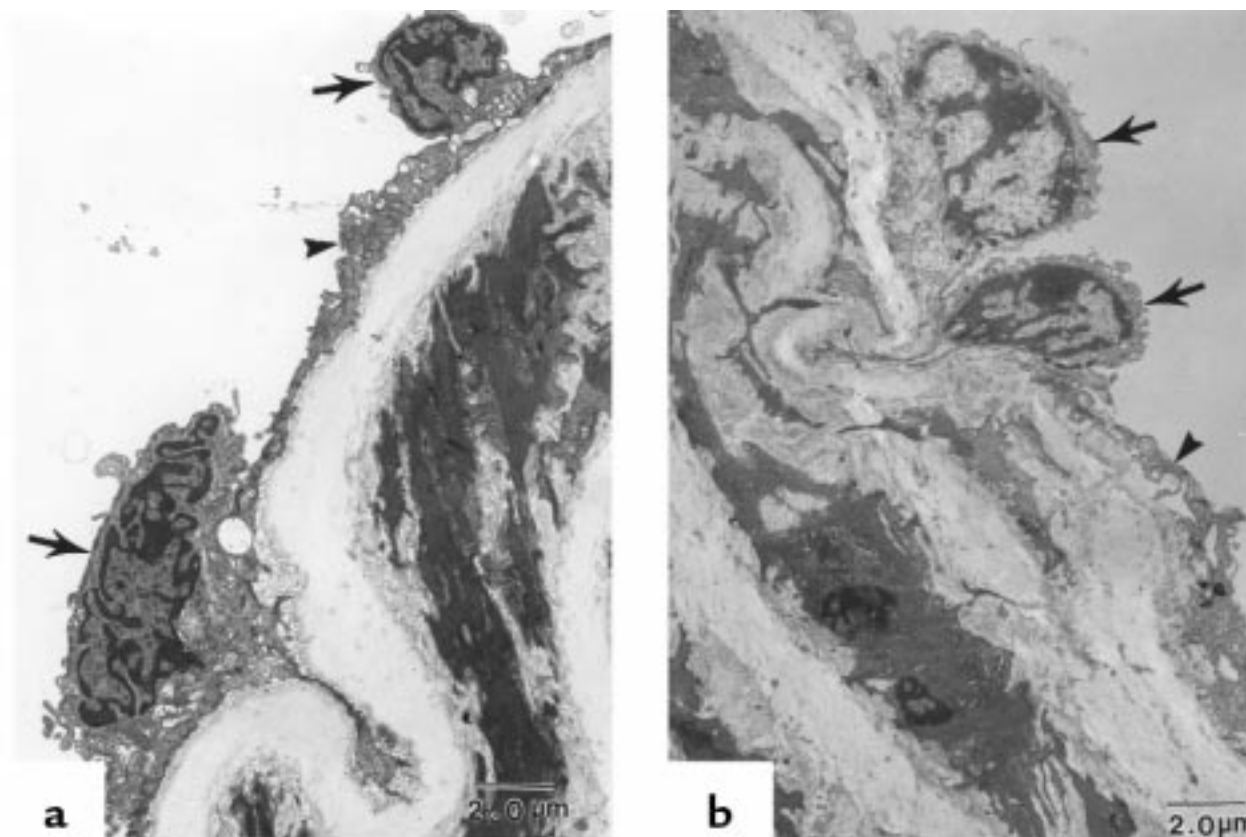
Figure 5
Thin-section electron micrographs (cross-sections) from the aortic arch of 5-week-old E0 (**a**) and E0/hA-I (**b**) mice. Arrows indicate monocytes adherent to the endothelial cell surface (arrowhead) and beginning their migration into the subendothelial space. ×5,280.
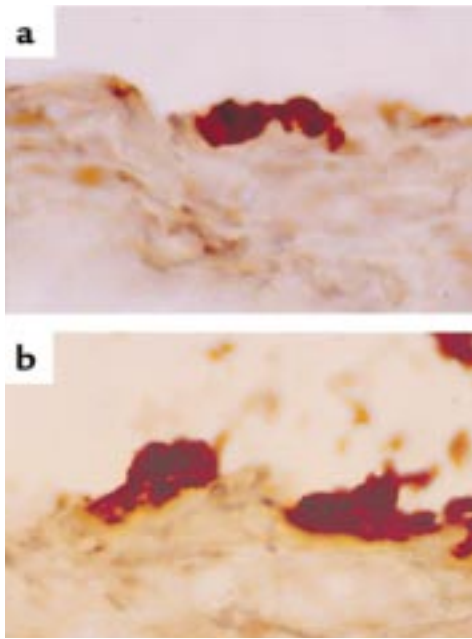
Figure 6

Aortic root sections from 8-week-old E0 and E0/hA-I mice. CD11a antibody staining (oil objective) demonstrating mononuclear cells bound to the vascular endothelium from E0 (**a**) and E0/hA-I (**b**) mice.

increased atherosclerosis in wild-type mice fed a high-fat, high-cholesterol diet (34). Therefore, it is possible that increases in paraoxonase could be associated with elevated apo A-I and HDL-C in E0/hA-I mice and could inhibit lipoprotein oxidation and atherosclerosis. In the present study, increased serum paraoxonase activity did not accompany increases in apo A-I and HDL-C in 8-week-old E0/hA-I mice. It is possible that differences in serum paraoxonase may be present in older E0 and E0/hA-I mice. A study by Aviram et al. (35) demonstrated that serum paraoxonase activity decreases in apo E–deficient mice after 3 months of age, coincident with increases in aortic lesion area and serum lipid peroxidation. In the presence of the human apo A-I transgene, this decrease in serum paraoxonase activity may not occur. Although we did not detect differences in serum paraoxonase activity in 8-week-old mice, HDL-C may still act as an antioxidant in the microenvironment of the vessel wall.

The present study indicates that elevated apo A-I and HDL-C inhibit macrophage foam cell formation at a stage following lipid retention, endothelial VCAM-1 induction, and monocyte adherence. Even though we could not exclude the possibility that apo A-I may affect the chemical composition of retained lipid, or its tendency to undergo oxidative modification, subsequent events such as endothelial induction of VCAM-1 and monocyte recruitment, which may depend upon the generation of bioactive oxidized lipids in the intima, were unaffected by the human apo A-I transgene. Several hypotheses can be constructed to explain how the human apo A-I transgene dramat-

ically attenuates foam cell formation despite the lack of an effect on lipid retention, endothelial activation, and monocyte adherence. First, apo A-I and HDL-C may interfere with monocyte/macrophage trafficking in the subendothelial space. HDL-C may inhibit production of vascular chemokines that may be necessary for the survival and retention of subendothelial macrophages. Second, apo A-I may affect lipoprotein loading of macrophages by affecting macrophage differentiation and/or scavenger receptor expression. Third, elevated apo A-I and HDL-C could promote reverse cholesterol transport, decrease foam cell formation, and possibly promote macrophage egress from the vessel wall. Presently, there are no assays that directly measure reverse cholesterol transport from the vessel wall in vivo. Stein et al (36) demonstrated that resorption of an intramuscular cholesterol depot is delayed in apo A-I–deficient mice. However, this phenomenon was abolished by dexamethasone, suggesting that this phenomenon was mediated by an inflammatory response and not by changes in reverse cholesterol transport (37).

In summary, we have shown that the human apo A-I transgene attenuates lesion formation in apo E–deficient mice at a stage following lipid retention, endothelial activation, and monocyte binding. Further in vivo studies are necessary to determine whether elevated HDL-C promotes cholesterol efflux from the vessel wall (reverse cholesterol transport theory) or affects monocyte/macrophage trafficking or lipoprotein oxidation (direct protection theory). The discovery of this mechanism will, we hope, provide targets for therapeutic agents designed to mimic the antiatherogenic actions of elevated HDL-C.
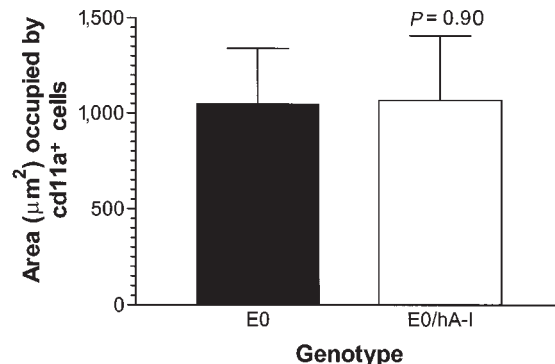
Figure 7

Quantification of CD11a antibody staining of bound mononuclear cells in the aortic root of apo E–deficient mice. The area occupied by stained cells was measured on five sections, obtained from an anatomically defined area of the aortic root from E0 (*n* = 7) and E0/hA-I (*n* = 7) mice. The mean of the areas from the 5 sections was then calculated for each mouse. Values are expressed as mean ± SEM for each group of mice.

1. Johnson, W.J., Mahlberg, F.H., Rothblat, G.H., and Phillips, M.C. 1991. Cholesterol transport between cells and high-density lipoproteins. *Biochim. Biophys. Acta.* **1085**:273–298.
2. Pillarisetti, S., Paka, L., Obunike, J.C., Berglund, L., and Goldberg, I.J. 1997. Subendothelial retention of lipoprotein (a). Evidence that reduced heparan sulfate promotes lipoprotein binding to subendothelial matrix. *J. Clin. Invest.* **100**:867–874.
3. Cockerill, G.W., Rye, K.A., Gamble, J.R., Vadas, M.A., and Barter, P.J. 1995. High-density lipoproteins inhibit cytokine-induced expression of endothelial cell adhesion molecules. *Arterioscler. Thromb. Vasc. Biol.* **15**:1987–1994.
4. Navab, M., et al. 1997. Mildly oxidized LDL induces an increased apolipoprotein J/paraoxonase ratio [published erratum appears in *J. Clin. Invest.* 1997. **99**:3043]. *J. Clin. Invest.* **99**:2005–2019.
5. Plump, A.S., Scott, C.J., and Breslow, J.L. 1994. Human apolipoprotein A-I gene expression increases high density lipoprotein and suppresses atherosclerosis in the apolipoprotein E-deficient mouse. *Proc. Natl. Acad. Sci. USA.* **91**:9607–9611.
6. Paszty, C., Maeda, N., Verstuyft, J., and Rubin, E.M. 1994. Apolipoprotein AI transgene corrects apolipoprotein E deficiency-induced atherosclerosis in mice. *J. Clin. Invest.* **94**:899–903.
7. Plump, A.S., et al. 1992. Severe hypercholesterolemia and atherosclerosis in apolipoprotein E-deficient mice created by homologous recombination in ES cells. *Cell.* **71**:343–353.
8. Zhang, S.H., Reddick, R.L., Piedrahita, J.A., and Maeda, N. 1992. Spontaneous hypercholesterolemia and arterial lesions in mice lacking apolipoprotein E. *Science.* **258**:468–471.
9. Nakashima, Y., Plump, A.S., Raines, E.W., Breslow, J.L., and Ross, R. 1994. ApoE-deficient mice develop lesions of all phases of atherosclerosis throughout the arterial tree. *Arterioscler. Thromb.* **14**:133–140.
10. Reddick, R.L., Zhang, S.H., and Maeda, N. 1994. Atherosclerosis in mice lacking apo E. Evaluation of lesional development and progression [published erratum appears in *Arterioscler. Thromb.* 1994. 14:**839**]. *Arterioscler. Thromb.* **14**:141–147.
11. Walsh, A., Ito, Y., and Breslow, J.L. 1989. High levels of human apolipoprotein A-I in transgenic mice result in increased plasma levels of small high density lipoprotein (HDL) particles comparable to human HDL3. *J. Biol. Chem.* **264**:6488–6494.
12. Rubin, E.M., Ishida, B.Y., Clift, S.M., and Krauss, R.M. 1991. Expression of human apolipoprotein A-I in transgenic mice results in reduced plasma levels of murine apolipoprotein A-I and the appearance of two new high density lipoprotein size subclasses. *Proc. Natl. Acad. Sci. USA.* **88**:434–438.
13. Tamminen, M., Mottino, G., Qiao, J.H., Breslow, J.L., and Frank, J.S. 1999. Ultrastructure of early lipid accumulation in apoE-deficient mice. *Arterioscler. Thromb. Vasc. Biol.* **19**:847–853.
14. Nakashima, Y., Raines, E.W., Plump, A.S., Breslow, J.L., and Ross, R. 1998. Upregulation of VCAM-1 and ICAM-1 at atherosclerosis-prone sites on the endothelium in the ApoE-deficient mouse. *Arterioscler. Thromb. Vasc. Biol.* **18**:842–851.
15. Piedrahita, J.A., Zhang, S.H., Hagaman, J.R., Oliver, P.M., and Maeda, N. 1992. Generation of mice carrying a mutant apolipoprotein E gene inactivated by gene targeting in embryonic stem cells. *Proc. Natl. Acad. Sci. USA.* **89**:4471–4475.
16. Dansky, H.M., Charlton, S.A., Harper, M.M., and Smith, J.D. 1997. T and B lymphocytes play a minor role in atherosclerotic plaque formation in the apolipoprotein E-deficient mouse. *Proc. Natl. Acad. Sci. USA.* **94**:4642–4646.
17. Nievelstein, P.F., Fogelman, A.M., Mottino, G., and Frank, J.S. 1991. Lipid accumulation in rabbit aortic intima 2 hours after bolus infusion of low density lipoprotein. A deep-etch and immunolocalization study of ultrarapidly frozen tissue. *Arterioscler. Thromb.* **11**:1795–1805.
18. Nievelstein-Post, P., Mottino, G., Fogelman, A., and Frank, J. 1994. An ultrastructural study of lipoprotein accumulation in cardiac valves of the rabbit. *Arterioscler. Thromb.* **14**:1151–1161.
19. Daugherty, A., et al. 1997. The effects of total lymphocyte deficiency on the extent of atherosclerosis in apolipoprotein E–/– mice. *J. Clin. Invest.* **100**:1575–1580.
20. Roselaar, S.E., Kakkanathu, P.X., and Daugherty, A. 1996. Lymphocyte populations in atherosclerotic lesions of apoE –/– and LDL receptor –/– mice. Decreasing density with disease progression. *Arterioscler. Thromb. Vasc. Biol.* **16**:1013–1018.
21. Zhou, X., Stemme, S., and Hansson, G.K. 1996. Evidence for a local immune response in atherosclerosis. CD4+ T cells infiltrate lesions of apolipoprotein-E-deficient mice. *Am. J. Pathol.* **149**:359–366.
22. Camejo, G., Hurt-Camejo, E., Wiklund, O., and Bondjers, G. 1998. Association of apo B lipoproteins with arterial proteoglycans: pathological significance and molecular basis. *Atherosclerosis.* **139**:205–222.
23. Khan, B.V., Parthasarathy, S.S., Alexander, R.W., and Medford, R.M. 1995. Modified low density lipoprotein and its constituents augment cytokine- activated vascular cell adhesion molecule-1 gene expression in human vascular endothelial cells. *J. Clin. Invest.* **95**:1262–1270.
24. Marui, N., et al. 1993. Vascular cell adhesion molecule-1 (VCAM-1) gene transcription and expression are regulated through an antioxidant-sensitive mechanism in human vascular endothelial cells. *J. Clin. Invest.* **92**:1866–1874.
25. Baker, P.W., Rye, K.A., Gamble, J.R., Vadas, M.A., and Barter, P.J. 1999. Ability of reconstituted high density lipoproteins to inhibit cytokine-induced expression of vascular cell adhesion molecule-1 in human umbilical vein endothelial cells. *J. Lipid Res.* **40**:345–353.
26. Ashby, D.T., et al. 1998. Factors influencing the ability of HDL to inhibit expression of vascular cell adhesion molecule-1 in endothelial cells. *Arterioscler. Thromb. Vasc. Biol.* **18**:1450–1455.
27. Kume, N., Cybulsky, M.I., and Gimbrone, M.A., Jr. 1992. Lysophosphatidylcholine, a component of atherogenic lipoproteins, induces mononuclear leukocyte adhesion molecules in cultured human and rabbit arterial endothelial cells. *J. Clin. Invest.* **90**:1138–1144.
28. Smith, J.D., et al. Decreased atherosclerosis in mice deficient in both macrophage colony-stimulating factor (op) and apolipoprotein E. *Proc. Natl. Acad. Sci. USA.* **92**:8264–8268.
29. Qiao, J.H., et al. 1997. Role of macrophage colony-stimulating factor in atherosclerosis: studies of osteopetrotic mice. *Am. J. Pathol.* **150**:1687–1699.
30. Gu, L., et al. 1998. Absence of monocyte chemoattractant protein-1 reduces atherosclerosis in low density lipoprotein receptor-deficient mice. *Mol. Cell.* **2**:275–281.
31. Palinski, W., et al. 1994. ApoE-deficient mice are a model of lipoprotein oxidation in atherogenesis. Demonstration of oxidation-specific epitopes in lesions and high titers of autoantibodies to malondialdehyde-lysine in serum. *Arterioscler. Thromb.* **14**:605–616.
32. Boullier, A., et al. 1995. Detection of autoantibodies against oxidized low-density lipoproteins and of IgG-bound low density lipoproteins in patients with coronary artery disease. *Clin. Chim. Acta.* **238**:1–10.
33. Watson, A.D., et al. 1995. Protective effect of high density lipoprotein associated paraoxonase. Inhibition of the biological activity of minimally oxidized low density lipoprotein. *J. Clin. Invest.* **96**:2882–2891.
34. Shih, D.M., et al. 1998. Mice lacking serum paraoxonase are susceptible to organophosphate toxicity and atherosclerosis. *Nature.* **394**:284–287.
35. Aviram, M., et al. 1998. Paraoxonase inhibits high-density lipoprotein oxidation and preserves its functions. A possible peroxidative role for paraoxonase. *J. Clin. Invest.* **101**:1581–1590.
36. Stein, O., et al. 1997. Delayed loss of cholesterol from a localized lipoprotein depot in apolipoprotein A-I-deficient mice. *Proc. Natl. Acad. Sci. USA.* **94**:9820–9824.
37. Stein, O., et al. Dexamethasone impairs cholesterol egress from a localized lipoprotein depot in vivo. *Atherosclerosis.* **137**:303–310.